Rheological and Viscoelastic Behavior of HDPE/Octamethyl-POSS Nanocomposites

M. Joshi,*,† B. S. Butola,† George Simon,‡ and Natalia Kukaleva‡

Department of Textile Technology, Indian Institute of Technology, Delhi, New Delhi 110016, India, and School of Physics and Materials Science, Monash University, Victoria 3800, Australia

Received June 25, 2005; Revised Manuscript Received December 21, 2005

ABSTRACT: Octamethyl-POSS−HDPE nanocomposites were prepared by the melt mixing route. The rheological and viscoelastic behavior of HDPE−octamethyl-POSS nanocomposites was investigated with a strain-controlled rheometer and dynamic mechanical analysis (DMA). The rheological results show that while at lower filler concentration (0.25−0.5 wt %) POSS particles act as lubricant and reduce the complex viscosity of the nanocomposites, at higher concentrations, viscosity increases. POSS remains miscible in HDPE at lower concentrations and lower temperatures used in the study; however it starts aggregating at higher concentrations and higher temperatures. The presence of POSS particles causes gelation in HDPE matrix at concentrations higher than 5 wt % possibly due to the segregated particle−particle interaction. The storage modulus shows an increase at lower POSS concentrations but decreases at higher POSS concentrations. The α-transition temperatures shift to higher values at low POSS concentrations and is attributed to restriction of the movement of HDPE chain segments in the intercrystalline regions due to the presence of POSS macromers around the crystallite boundaries. The effect of POSS on morphology of HDPE was studied with X-ray diffraction and DSC techniques. It was observed that while POSS does not interfere with the crystallization of HDPE, it crystallizes itself into nanocrystals.

Introduction

The area of polymeric nanocomposites has invoked much interest in recent years. A nanocomposite may be defined as a polymer filled with nanofillers, at least one of whose dimensions is in the nanometer range (∼100 nm). These nanofillers have been found to improve the mechanical, barrier, electrical, and thermal properties of base polymer significantly at very low filler concentration compared to conventional macrocomposites. This has opened up possibilities for producing high-performance lightweight composites without compromising other properties such as optical behavior or weight. Most often, nanoclays, carbon nanofibers/nanotubes, and nanosilica have been the preferred fillers.[1,2] However, a new class of nanofiller, POSS (polyhedral oligomeric silsesquioxane), is emerging for use in nanostructured materials. POSS, essentially a hybrid material (organic−inorganic), contains a basic polyhedral silicone−oxygen nanostructured skeleton or cage, with a precisely defined Si−Si diameter of 0.53 nm. The cage may have 8 (a cubelike cage) or 12 Si atoms located at the corner of the cage, surrounded by 8 or 12 organic groups, respectively, with a ratio of Si:O of 2:3[3] (Figure 1). POSS chemistry is very versatile, and it is possible to attach different kinds of functional or nonfunctional organic groups (R) to the corner Si molecules for further reaction. The POSS molecule can thus be synthetically modified to contain functional groups which readily allow copolymerization, light sensitization, and improved solubility in organic solvents, and this sets it apart from other nanofillers. The incorporation of POSS cages into polymeric materials may result in dramatic improvements in polymer properties, including increase in upper use temperature, oxidative resistance, and surface hardening, leading to improved mechanical properties as well as a reduction in flammability.[4] These enhancements have been found to apply to a wide range of thermoplastics and some thermoset systems.[5]

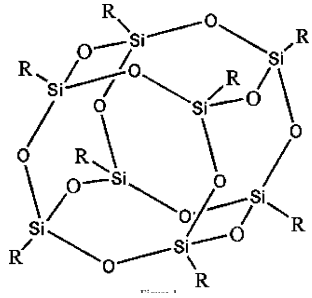

Figure 1. Molecular structure of POSS (R = any organic group).

While the bulk of POSS nanocomposite work has focused on the reactive type of POSS nanofiller, where the POSS moiety becomes an integral part of the polymeric chains, there have been much fewer studies on physically blended nonreactive POSS in polymer matrices.[6] With the increased availability of commercial POSS materials, the ability to include them in thermoplastic systems by conventional techniques is attractive. We have studied, for example, the crystallization behavior of octamethyl-POSS-filled high-density polyethylene (HDPE) nanocomposites prepared by the melt blending route.[7]

Although POSS molecules can be thought of as the smallest particles of silica possible, they are physically large with respect to polymer dimensions and nearly equivalent in size to most polymer segments and coils. Introduction of fillers can affect the morphology and change the rheological and viscoelastic behavior of the polymers by introducing filler−matrix interactive forces or restriction of polymer chain movement by filler particles. It is thus of much interest to study the rheological and viscoelastic behavior of polymers filled with nanosized fillers, where the nanoparticle size allows interactions with polymer at the molecular level. While there have been many studies on the effect of particulate fillers on polymer morphology,[8−10] there are relatively few studies[11] on the effect of

† Indian Institute of Technology.
‡ Monash University.
* Corresponding author. E-mail: mangala@textile.iitd.ernet.in.

10.1021/ma051357w CCC: $33.50
Published on Web 01/26/2006

Table 1. Processing Conditions for Melt Mixing of POSS and HDPE in Twin-Screw Extruder

barrel zone temp (°C)					
I	II	III	IV	die zone temp (°C)	screw RPM
165	185	215	225	240	60

Table 2. Composition of Various HDPE−POSS Nanocomposites

POSS content (wt %)	HDPE content (wt %)	nanocomposite code
0	100	HDPE
0.1	99.9	P01
0.25	99.75	P025
0.5	99.5	P05
1	99	P1
2	98	P2
3	97	P3
5	95	P5
10	90	P10

particulate nanofillers on morphology. In this study the rheological and dynamic mechanical behavior of HDPE−POSS nanocomposites has been studied and correlated to the morphology.

Experimental Section

Materials. The HDPE used in the study was provided by Reliance Industries Limited, India (Relene E 52009-Oriented Tape and monofilament grade) with an MFI of 0.9. The POSS used was octamethyl-POSS (MS 0830, where R = CH_3) supplied by Hybridplastics, Fountain Valley, CA.

Nanocomposite Preparation. The masterbatches of POSS in HDPE (1 and 10 wt % loading) were prepared on a twin-screw extruder (APV Baker, model MP 19 TC) by melt mixing. The processing conditions are given in Table 1. The 10 wt % POSS masterbatch was then used to prepare HDPE/POSS nanocomposite filaments of various compositions, the details of which are given in Table 2. The nanocomposite as-spun filaments were prepared by melt extrusion of HDPE and the masterbatch in suitable ratios to get the above-mentioned compositions in the laboratory single screw extruder (Betol, UK). The extrudate was solidified by quenching it in a water bath maintained at 12−14 °C. The optimized extrusion conditions are given in Table 3.

X-ray Diffraction. The characterization of neat POSS and POSS crystallites in HDPE was carried out on a Bruker Axs X-ray diffractometer (D8 Advanced) using Cu Kα radiation operated at 40 kV and 30 mA. The data were collected in 2θ angle range 2−30° at a scanning rate of 0.5°/min.

The weight fraction crystallinity of the nanocomposite filaments was determined by superimposing the amorphous curve on the $I(\theta)$ vs θ diffraction scans obtained from the X-ray diffractometer and using the following formula after segregating the crystalline contribution:

$$X_c = \frac{\int_0^\alpha s^2 I_c(s)\,ds}{\int_0^\alpha s^2 I_s(s)\,ds} \quad (1)$$

where X_c = crystalline mass fraction, $s = 2 \sin\theta/\lambda$, I_c = crystalline diffraction intensity, I_s = total diffraction intensity, $\lambda = 1.54$ Å, and θ = Bragg's angle. The average lateral crystalline thickness is estimated from the broadening observed in the WAXD pattern recorded for 2θ range of 2−30°, at a scanning rate of 0.5°/min. The integral breadth of the diffraction intensity arising from the imperfection of crystallites is measured in terms of $\beta_{1/2}(hkl)$. The higher the value of $\beta_{1/2}(hkl)$, the lower is the crystalline perfection.

The apparent crystalline size was determined according to Scherrer's equation:

$$D_{(hkl)} = \frac{K\lambda}{\beta \cos\theta} \quad (2)$$

where β is the half-width of the diffraction peak in radians, K is equal to 0.9, θ is the Bragg angle, and λ is the wavelength of the X-rays. The values of $D_{(hkl)}$ for (110) reflection were calculated.

Differential Scanning Calorimetry. DSC studies were carried out on a Perkin-Elmer Pyris-1 differential scanning calorimeter in a flowing nitrogen atmosphere. The samples were run in triplicates to ensure reproducibility. The scans were obtained from 50 to 160 °C at a heating rate of 10 °C/min with sample weight around 5 mg. The onset, end, and peak melting temperatures, as well as heat of fusion (ΔH), were calculated from the scans using built-in software. The crystallinity of the samples was calculated using the following relationship:

$$X_{DSC} = \Delta H_{sample}/293$$

Rheological Analysis. Circular disklike samples with 25 mm diameter and 2 mm thickness were prepared on a compression-molding machine (Carver Press). The chopped HDPE−POSS nanocomposite as-spun filaments were filled in a mold with cavities having similar dimensions as the specimen. The filled mold was placed between two polished stainless steel sheets and put in the compression-molding machine set at a temperature of 180 °C. The specimens were formed at 3 ton pressure for 3 min, cooled to 80 °C by circulating water, and taken out. Rheological studies were carried out on controlled strain rheometer, ARES. Measurements were performed in the plate−plate configuration with a gap of 1.8−2.0 mm.

Strain sweeps within the range of $\gamma = 0-40\%$ were done on the neat HDPE, as well as on 0.25%, 0.5% 1%, 2%, 5%, and 10% POSS nanocomposites at three temperatures: 180, 190, and 200 °C. At $\omega = 10$ rad/s, the most sensitive rheological parameter, G', was found to be stable at $\gamma < 15-20\%$. For this reason, the dynamic (frequency sweep) tests were performed at $\gamma = 10\%$.

Storage modulus (G'), loss modulus (G''), and complex viscosity (η^*) were measured in the frequency sweep experiments performed over a frequency range of 0.1−100 rad/s, with data collected at five points per decade. The η', the real part of the complex viscosity, the η'', the imaginary part of the complex viscosity, the δ, delta, and G^*, complex modulus, were calculated according to the following equations:

$$\eta' = G''/\omega \quad (3)$$

$$\eta'' = G'/\omega \quad (4)$$

$$\delta = \text{atan}\, G''/G' \quad (5)$$

and

$$|G^*| = \{(G'^2 + G''^2)^{1/2}\} \quad (6)$$

Dynamic Mechanical Characterization. The nanocomposite filaments for the study of viscoelastic behavior were prepared by drawing the as-spun filaments in two stages. The optimized drawing conditions are given in Table 3. Viscoelastic studies were carried out by dynamic mechanical analysis of the filaments using a Perkin-Elmer DMA7e instrument in tensile mode. A temperature range

Table 3. Extrusion and Drawing Conditions for Filament Preparation on Single-Screw Extruder

barrel zone temp (°C)	die zone temp (°C)	screw RPM	drawing zone I		drawing zone II	
			drawing temp (°C)	draw ratio	drawing temp (°C)	draw ratio
210, 230, 250	270	6	100	6	110	1.5

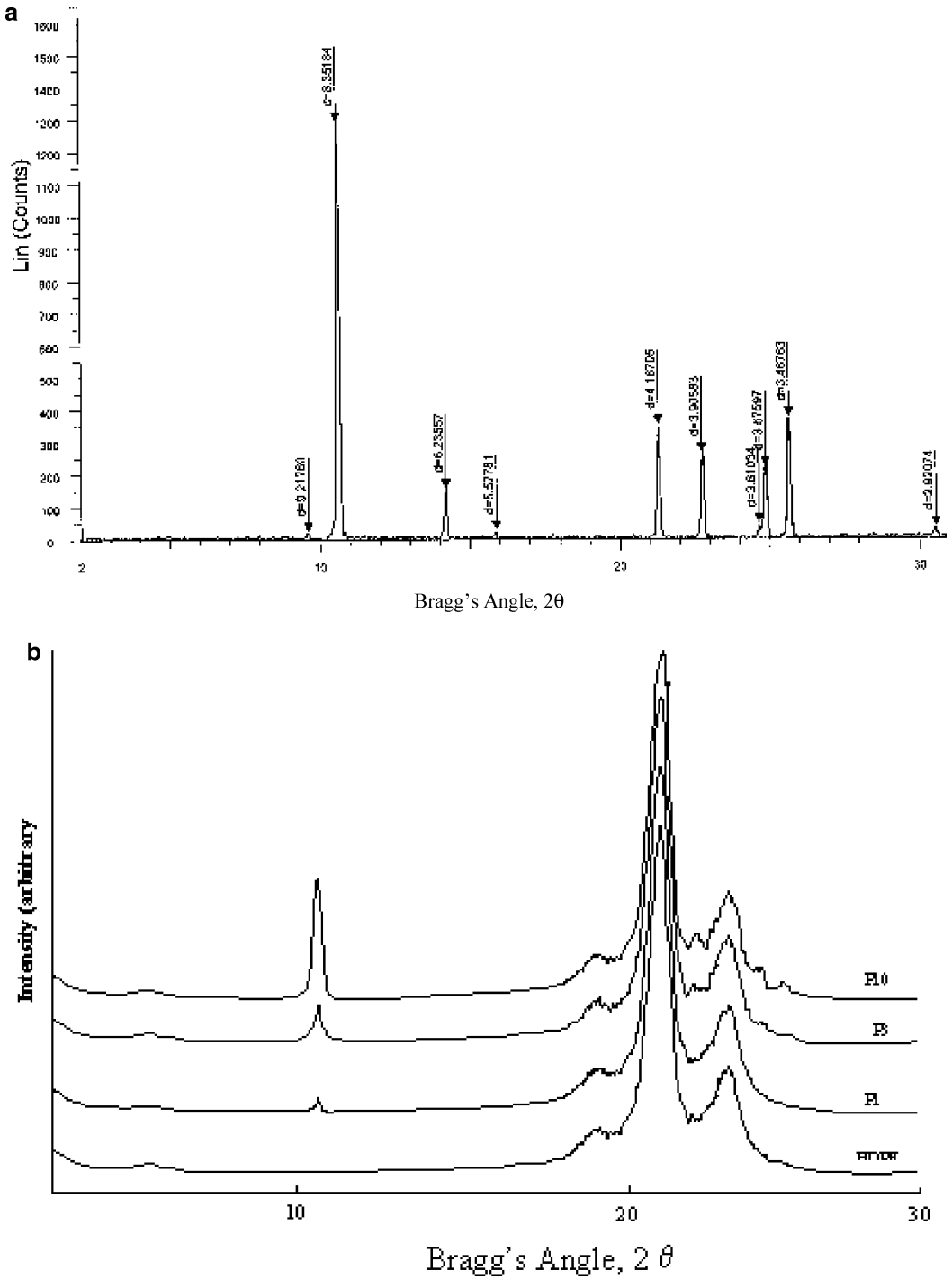

Figure 2. (a) X-ray diffraction patterns of neat POSS. (b) X-ray diffraction patterns of HDPE and HDPE−POSS nanocomposites.

from −80 to 120 °C at a heating rate of 5 °C/min and frequency of 1 Hz was used, after the optimization of the static and dynamic loads.

Results and Discussion

Morphology. X-ray Diffraction. Figure 2a,b shows the X-ray diffraction patterns of the POSS, HDPE, and selected HDPE−POSS nanocomposite filaments (1−10 wt %) with Bragg's angle (2θ) varying from 2° to 30°. Neat HDPE shows two sharp characteristic peaks at 21.3° and 23.5°, which are assigned to the 110 and 200 reflections of the Bunn orthorhombic subcell. These values agree well with the values reported for polyethylene as 21.4° and 23.68° and 21.62° and 23.94° by Murthy et al.[12] and Russell et al.,[13] respectively. The diffraction patterns for the HDPE−POSS nanocomposites are similar to that of neat HDPE, and it is evident from the figure that the basic nature of the diffraction pattern does not change in the presence of POSS.

The position of 110 and 200 peaks for nanocomposites are very similar to that of neat HDPE. The determination of crystallinity was done by taking the peak of amorphous halo[12,13] at 20°. Table 4 shows the values of crystallinity parameters for HDPE and HDPE−POSS nanocomposite filaments calculated using eqs 1 and 2. It is clear from the values of crystallinity and crystal size that the presence of POSS up to 5 wt % does not interfere with the development of crystallinity of HDPE polymer. The crystal size (thickness) also remains unchanged. However, the peak at 23.5° does become less intense at 10 wt % POSS; crystallinity values are also marginally low as

Table 4. Value of Crystalline Parameters for HDPE and Nanocomposites from X-ray Data

sample no.	sample	% crystallinity	crystal thickness (nm)
1	HDPE	74	128
2	P0.1	75	127
3	P0.25	75	126
4	P0.5	74	125
5	P1	74	127
6	P2	74	126
7	P5	73	120
8	P10	71	108

Table 5. Melting Parameters for HDPE and HDPE−POSS Nanocomposites from DSC Studies

sample	crystal size (nm)
neat POSS	40
P3	25
P10	25

compared to neat HDPE, which means that crystallization of HDPE is affected at POSS content of 10 wt %.

Since crystallinity of HDPE is not affected by presence of POSS up to 5 wt %, it can be assumed that POSS is dispersed mostly in the amorphous domains of HDPE matrix. From Figure 2a it can be observed that the POSS is a highly crystalline material and has a characteristic dominant diffraction peak near 10.5°. In Figure 2b it is observed that a peak corresponding to the dominant POSS peak just appears at 1 wt % POSS content and grows progressively with increase in the content of POSS in HDPE. This means that POSS molecules exist as crystals in HDPE matrix at POSS concentrations just over 1 wt %. Zheng et al.[14] reported that POSS is able to crystallize in nanocomposites even when it is a part of the polymeric chain and there are restrictions on its movement. In a recent study Fu et al.[6] have reported that POSS retains its crystalline structure in EP copolymer matrix even at a temperature of 200 °C.

Hence, it is obvious that POSS is able to crystallize when it is dispersed physically in HDPE matrix, and there are no chemical linkages to restrict its movement. It means up to 1 wt % POSS is almost completely dispersible in HDPE matrix, and at higher concentrations it starts agglomerating and crystallizing. This is also supported by the rheological analysis of the miscibility of HDPE and POSS discussed later in this article. Another observation that can be made from the diffractograms is that the peaks are not as sharp as neat POSS peaks. This means that the dispersed POSS crystals are not as perfect as neat POSS crystals. It can be inferred that these crystallites are formed from the dispersed POSS particles, and although the process of melt mixing is able to disperse the POSS at nano/molecular level in HDPE matrix, eventually POSS manages to crystallize when concentration levels increase beyond 1 wt %. The size of the POSS crystals is given in Table 5. It is clear from the results that crystals from dispersed POSS in nanocomposites are smaller than the neat POSS crystals.

Differential Scanning Calorimetry. DSC is another investigative tool to obtain useful information about the crystallinity and crystal size. The typical melting parameters like onset, end, and peak melting temperatures and also the DSC crystallinity values (heat of fusion for 100% crystalline PE = 293 kJ/kg[15]) obtained from the melting endotherms are given in Table 6.

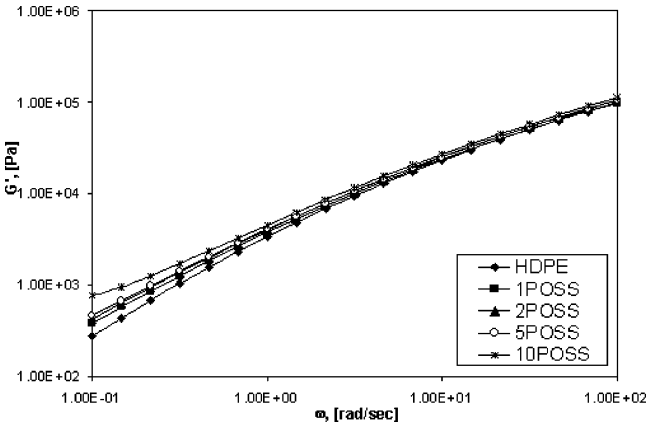

Figure 3. Storage moduli for HDPE−POSS nanocomposites measured at 190 °C.

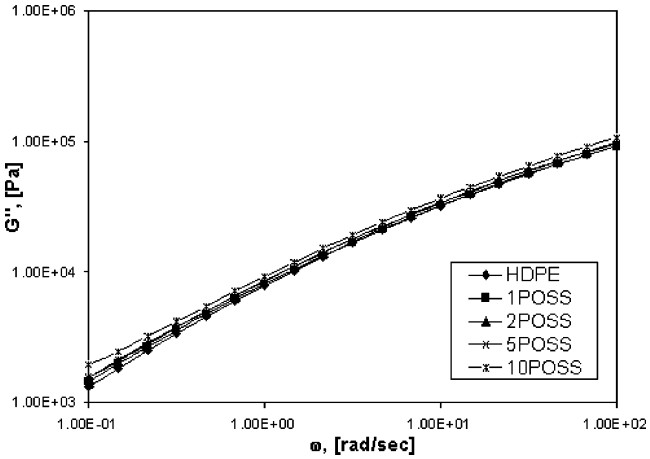

Figure 4. Loss moduli for POSS−HDPE nanocomposites measured at 190 °C.

The values for melting parameters and crystallinity indicate that there is no influence of POSS macromers on the crystallization of HDPE polymer up to 5 wt %. At 10 wt % POSS content, the peak melting temperature shifts to lower side by almost 2° as compared to neat HDPE as well as the crystallinity drops from 74% to 70%. This observation is in agreement with the findings of the X-ray study.

Rheological Analysis. The variation of G', G'', and η^* as a function of frequency at 190 °C for HDPE and HDPE/POSS nanocomposites is shown in Figures 3−5. It is observed that at all three temperatures, i.e., 180, 190, and 200 °C, storage modulus (G') and loss modulus (G'') of HDPE increase on addition of POSS, in proportion to the POSS concentration. However, the value of complex viscosity η^* drops at low POSS concentrations (0.25−0.5 wt %) and thereafter increases, with a further increase in POSS loadings (Figure 6a,b). It is also apparent that at a higher test temperature, i.e., 200 °C, a larger

Table 6. Flow Activation Energy E_a Values for HDPE/POSS Nanocomposites

sample no.	sample code	onset temp (melting), °C	end temp (melting), °C	peak temp (melting), °C	ΔH, J/g	% crystallinity
1	HDPE	132.6	140.7	138.3	214.7	73.3
2	P.25	132.6	140.2	137.7	219.8	75.2
3	P.5	132.2	140.3	138.0	219.5	75.3
4	P1	132.4	140.5	137.9	216.4	74.6
5	P3	132.2	140.3	137.7	210.7	74.1
6	P10	132.3	138.6	136.4	185.2	70.2

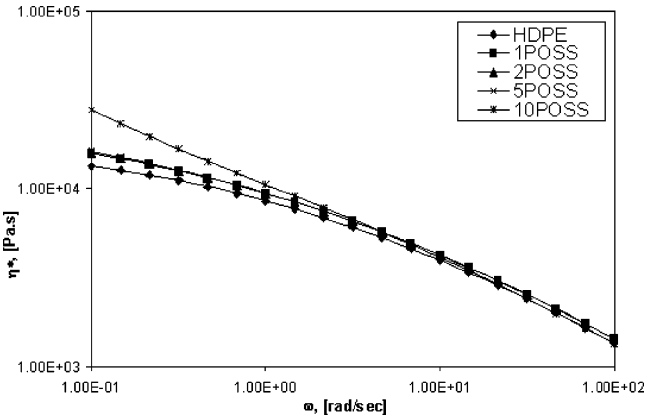

Figure 5. Complex viscosities for HDPE−POSS nanocomposites measured at 190 °C.

difference between G', G'', and η^* for neat HDPE and HDPE/POSS nanocomposites occurs. The miscibility at low concentrations (<1 wt %) likely leads to a fine dispersion with some level of PE chain−POSS interaction, i.e., weak van der Waals forces, and this could probably cause decreased chain entanglements and more free volume in the melt, thus resulting in lower complex viscosity (η^*). The increased drawability of these filaments supports this argument further. However, at higher POSS concentrations beyond ~2 wt %, it is not completely miscible at the molecular level and thus forms aggregates or nanocrystals which hinder the flow and thus raise the viscosity.

Cole−Cole and Van Gurp Analysis of Rheological Data. The rheological data are analyzed using the Cole−Cole plot, representing the relationship between the real (η') and the imaginary (η'') parts of complex viscosity. It has been reported that the plot can be used to analyze the miscibility of polymer blends.[16−20] A smooth, semicircular shape of the plotted curves would suggest good compatibility, i.e., phase homogeneity in the melt (ibid), and any deviation from this shape shows a nonhomogeneous dispersion and phase segregation due to immiscibility.

The Cole−Cole plots at 180 and 200 °C are shown in parts a and b of Figure 7, respectively. It appears that at 180 °C nanocomposites with 1, 2, and 5 wt % POSS are miscible (or at least finely dispersed), as is evident from the smooth, semicircular shape of the plots, while at 10 wt % POSS, there is a clear deviation which indicates immiscibility of POSS at 10 wt %. However, at 200 °C (Figure 7b), the 2, 5, and 10% POSS curves show upward inflections, which may be indicative of immiscibility or yield behavior.[21] The 10 wt % POSS composition is more immiscible than 2 and 5 wt % POSS-filled HDPE (the former likely being in the spinodal range and the latter between the binodal and spinodal composition). The 1% POSS nanocomposite does not show the upward inflection, as it is still miscible at 200 °C. However, diagnosing miscibility of blends merely from the shape of the Cole−Cole dependence (η'' vs η') could be misleading,[22] and other supporting rheological data are required to strengthen the hypothesis.

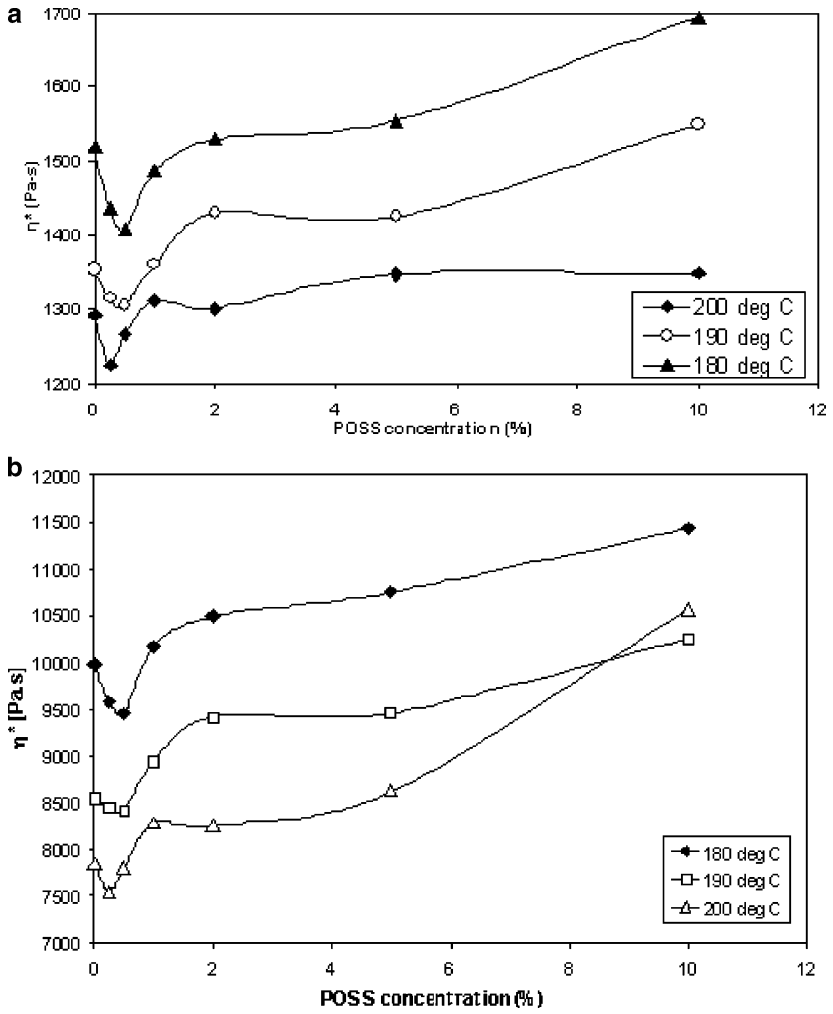

Figure 6. (a) Influence of composition on complex viscosities of HDPE−POSS nanocomposites at $\omega = 10.0$ rad/s. (b) Influence of composition on complex viscosities of HDPE−POSS nanocomposites at $\omega = 1$ rad/s.

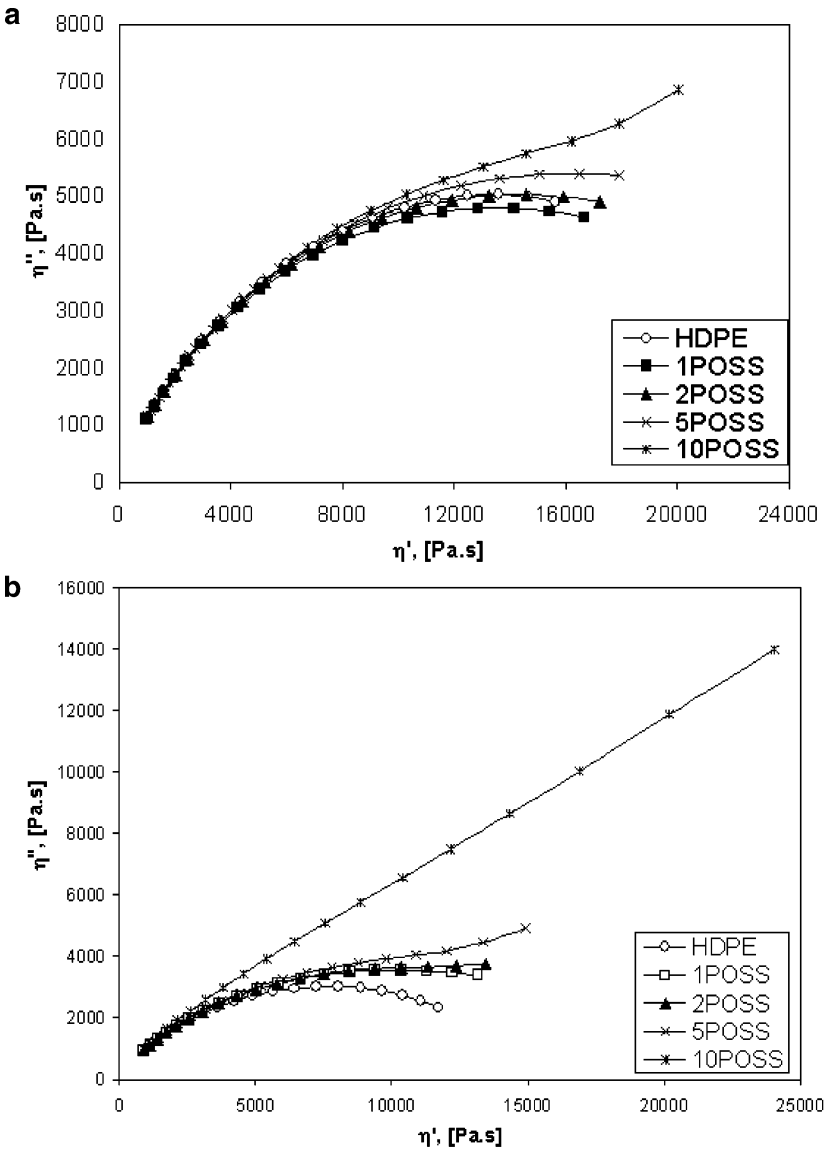

Figure 7. (a) Cole−Cole plots of the HDPE/POSS nanocomposites, $T = 180$ °C. (b) Cole−Cole plots of the HDPE/POSS nanocomposites, $T = 200$ °C.

The validity of the observation based on the Cole−Cole plots' appearance was further supported by the van Gurp's plots representing the relationship between the complex modulus (G^*) and delta (δ) (Figure 8). While the use of the Cole−Cole plot for assessing the polymer blends' miscibility is quite common,[16−22] there is little published data[23] on the use of the Van Gurp's plot. However, it has been reported that such plots have been useful for similar systems, such as for polymer matrices (PP) and inorganic fillers (synthetic clay). The Cole−Cole plots (η'' vs η') also tend usually to be applied for systems where two (or more) phases are polymers,[16−22] i.e., to the completely organic systems.

As can be seen from Figure 8, the time−temperature superposition principle (TTS) holds for the neat HDPE ($T =$ 180, 190, and 200 °C), nanocomposites containing 1 wt % of POSS ($T = 180$, 190, and 200 °C), and those containing 2 wt % of POSS for two lower temperatures only ($T = 180$ and 190 °C). The 2 wt % POSS composition at 200 °C and composites containing 5 and 10 wt % of POSS did not merge into the common curve. The deviation was particularly notable for the 10 wt % POSS composite at the highest experimental temperature of 200 °C. According to Reichert et al.,[23] the deviation indicates morphological changes taking place in the melt during the experiment. It is thus indicated that only the stable compositions up to 5 wt % POSS, which show isotherms merging into a common curve, are homogeneous or miscible.

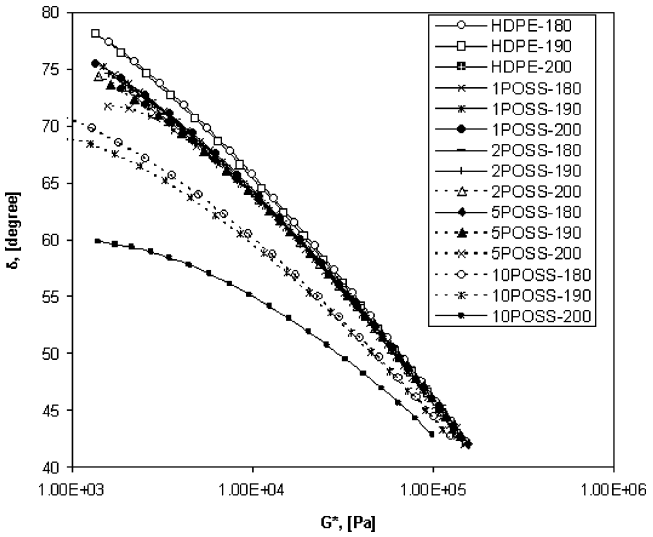

Figure 8. van Gurp's plots of HDPE−POSS nanocomposites.

CDV

Table 7

sample	activation energy (kJ/mol)	regression coefficient (R^2)
HDPE	26.2	0.99
1% HDPE−POSS	21.4	0.98
2% HDPE−POSS	22.2	0.99
5% HDPE−POSS	24.0	0.99

This agrees with the trends observed in the Cole−Cole plots (Figure 7a,b).

The compatibility of HDPE−POSS nanocomposites was assessed further using other previously proposed criteria for rheological compatibility of polymer blends proposed by Han and Chuang.[24,25] In these reports, experimental data for well-known miscible (compatible)/immiscible (incompatible) polymer pairs showed that G' vs G'' plots give (a) temperature-independent correlation for both compatible and incompatible blend systems, (b) composition-independent correlation for compatible blends, and (c) composition-dependent correlation for incompatible blends. The temperature dependency of G' vs G'' has also been used for determining the thermally induced order−disorder transition of block copolymers.[26−27] The theoretical justification based on molecular−thermodynamic arguments for assessing rheological compatibility of the blends has also been reported for polystyrene-*block*-polyisoprene copolymers.[27]

As expected, a temperature-independent correlation (G' vs G'') for neat HDPE and all composites up to 5 wt % POSS was observed. For sake of brevity, only graphs showing 1% POSS (Figure 7a), 5% POSS (Figure 7b), and 10% POSS (Figure 7c) nanocomposites are presented. But for 10% POSS nanocomposite, a temperature dependence was noticed (Figure 7c), which means that above 5% POSS content the nanocomposite starts behaving in an anomalous way and a phase separation of POSS and HDPE is indicated.

Temperature Dependence of Rheological Parameters: Effect of POSS. To express the viscosity−temperature behavior, an Arrhenius-type equation derived by Eyring[22] was used:

$$\eta = A e^{E_a/RT} \tag{7}$$

where η is the absolute or zero-shear viscosity, A is the constant, T is the absolute temperature, R is the gas constant, and E_a is the flow activation energy.

The activation energy (E_a) of the POSS nanocomposites as well as the neat HDPE was defined from the slopes of $\ln(\eta)$ plotted vs $1/T$. Determining the precise value of E_a for the HDPE−POSS nanocomposites is not the purpose of the study, and as such, complex viscosity, $\eta^*_\omega = 0.1$ rad/s, data (measured in the frequency sweep experiments) are used instead of zero-shear viscosity data and fitted into the equation

$$\ln(\eta_{\omega = 0.1\ \text{rad/s}}) = \ln A + \frac{E_a}{RT} \tag{8}$$

Regression analysis showed that the Arrhenius-type equation was applicable for all samples, giving $R^2 \geq 0.9876$, and the resultant calculated effective activation energy (E_a) values are shown in Table 7. The value of E_a for HDPE (26.2 kJ/mol) is in agreement with published values for this polymer,[28−30] which fall in the range from 26 to 28 kJ/mol. It is, thus, expected that E_a values for the HDPE−POSS nanocomposites (using complex viscosities at $\omega = 0.1$ rad/s) calculated from the plots are also valid. The values of E_a for POSS nanocomposites are lower than that of neat HDPE. It appears that the POSS at the very low concentrations serves as a lubricant for HDPE, reducing resistance to flow of this polymer. As the content of POSS increases further, it aggregates and physically hinders the flow; hence, E_a increases slightly but is still lower than neat HDPE. Another explanation is that at 1 wt % concentration POSS is completely miscible in the HDPE matrix, and because of very small nanometer dimensions, it interferes with chain entanglement and increases free volume in the melt and leads to lowering of the activation energy.[28] The compositions containing less than 2 wt % of POSS is completely miscible with the matrix polymer. The excess of POSS (~5 wt %) would be immiscible in HDPE matrix and, correspondingly, would hinder the flow and thus raise the activation energy of the nanocomposites. However, Fu et al.,[6] in their study on POSS with EP copolymers, do not find any change in the activation energy parameter of the nanocomposites. This may be due to less intense POSS−polymer interactions in POSS−EP copolymer system of Fu et

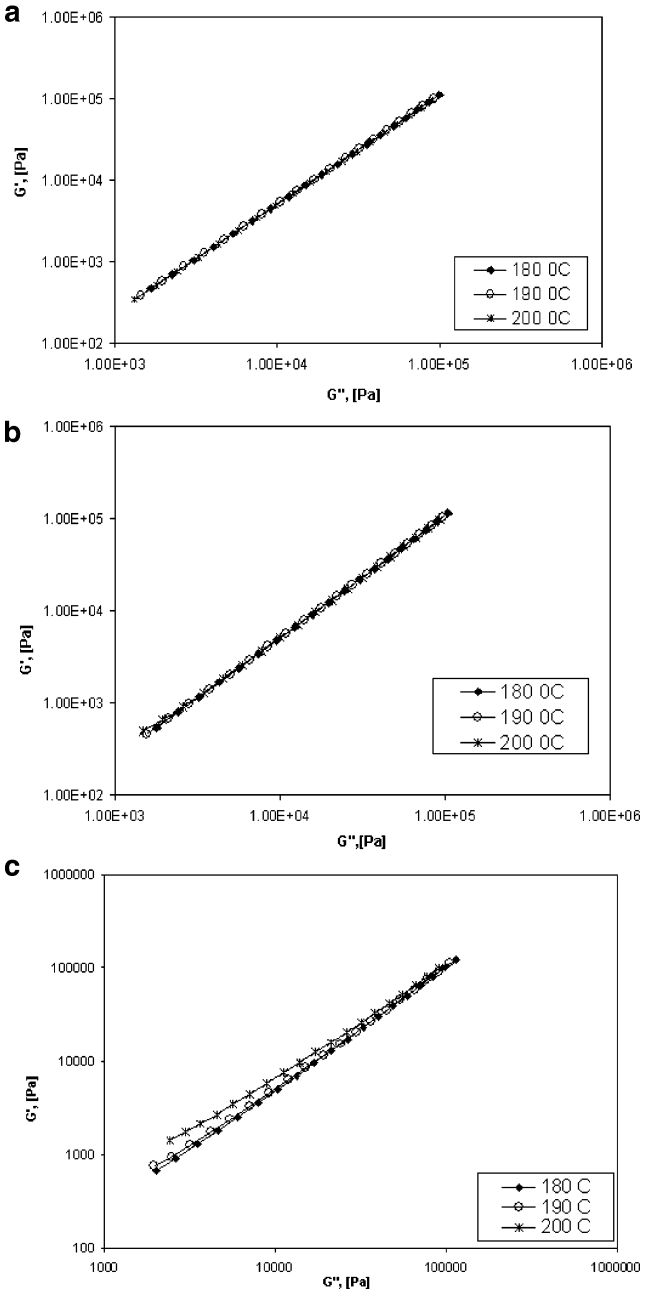

Figure 9. (a) G' vs G'' for HDPE/POSS (1 wt %) nanocomposites at different temperatures. (b) G' vs G'' for HDPE/POSS (5 wt %) nanocomposites at different temperatures. (c) G' vs G'' for HDPE/POSS (10 wt %) nanocomposites at different temperatures.

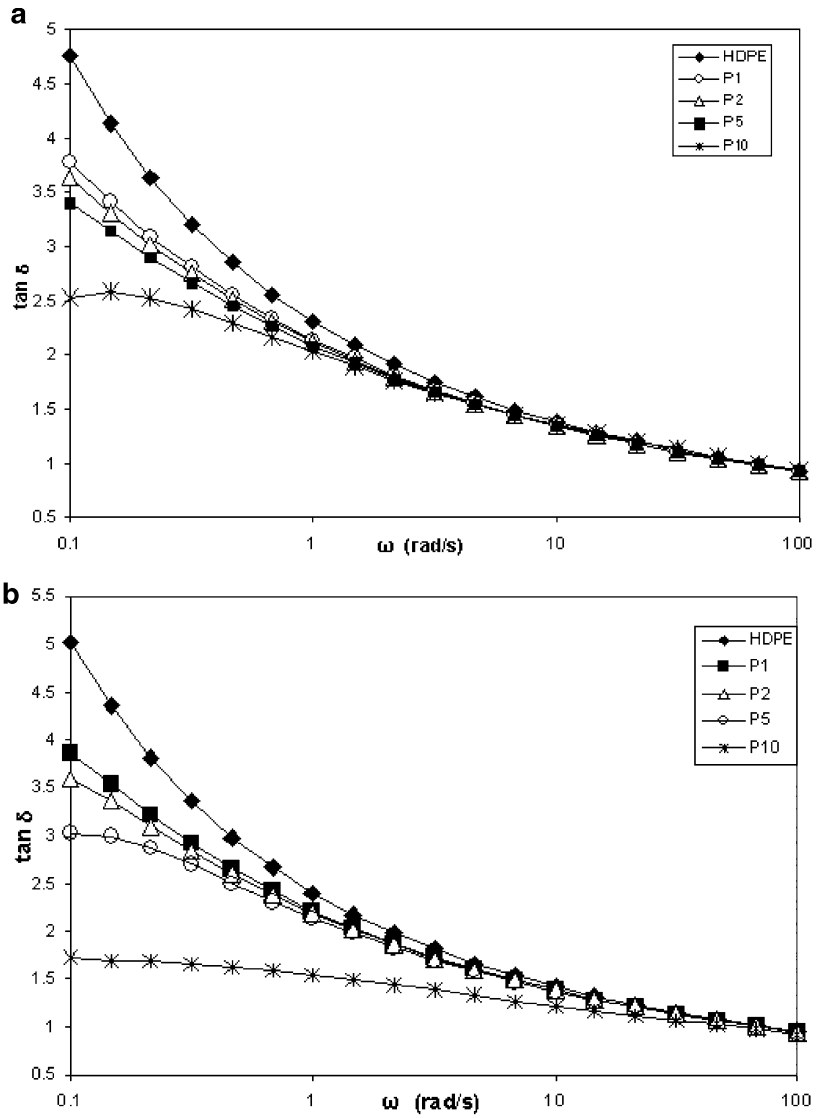

Figure 10. (a) tan δ vs ω plots for HDPE and HDPE−POSS nanocomposites at 190 °C. (b) tan δ vs ω plots for HDPE and HDPE−POSS nanocomposites at 200 °C.

al.[6] as compared to the molecularly dispersed POSS in the present system.

Physical Gelation in HDPE: Role of POSS. In a related study, Fu et al.[6] reported a physical gelation phenomenon in ethylene propylene (EP) melts induced by POSS molecules. A polymeric gel can be defined as a 3-dimensional network where polymer chains are bound by physical or chemical cross-links. Since the HDPE−POSS nanocomposites system used in this study is similar to the POSS−EP system, the possibility of physical gelation in HDPE melts due to POSS molecules was also investigated.

Fu et al.[6] used a simple approach in their work, which was based on the results from Winter,[31−34] who showed that at gel point the rheological behavior of a polymer could be characterized by "self-similar relaxation pattern". The viscoelastic parameters for a critical gel were shown to be related as

$$G'_c(\omega) = \frac{G''_c(\omega)}{\tan(n\pi/2)} = S\Gamma(1-n)\cos(n\pi/2)\omega^n \qquad (9)$$

where $\Gamma(1-n)$ is the gamma function, n is the relaxation exponent whose value lies between 0 and 1, ω is the angular frequency, and G'_c and G''_c are storage and loss moduli at the gel point.

At the critical gel point the ratio between G'_c and G''_c becomes frequency independent, i.e.

$$\tan\delta_c = \frac{G''_c}{G'_c} = \tan\left(\frac{n\pi}{2}\right), \quad \text{where } 0 < \omega < 1/\lambda_0 \qquad (10)$$

where λ_0 is the relaxation time of the transition from rubbery plateau to the reptation regime in the low-frequency zone. This typical characteristic of the critical gel provides one with an easy tool for determination of gel point using rheological methods. Hence, in a tan δ vs ω plot, the gel point will manifest itself by the appearance of a plateau with zero slope.

Typically, for polymer melts the slopes of curves in a tan δ vs ω plot are negative while for the solids (gels) it is positive. Hence, the transition from melt to gel can be easily identified if a change from negative to positive slope occurs in a tan δ vs ω plot. Figure 10a,b shows the tan δ vs ω plots for HDPE and HDPE−POSS nanocomposites at 190 and 200 °C. It is observed that the rheological behavior of neat HDPE has a negative slope over the frequency range tested and increases with increase in frequency. This behavior is typical of polymer melts. With incorporation of POSS in HDPE matrix, the slope starts increasing in the low-frequency region.

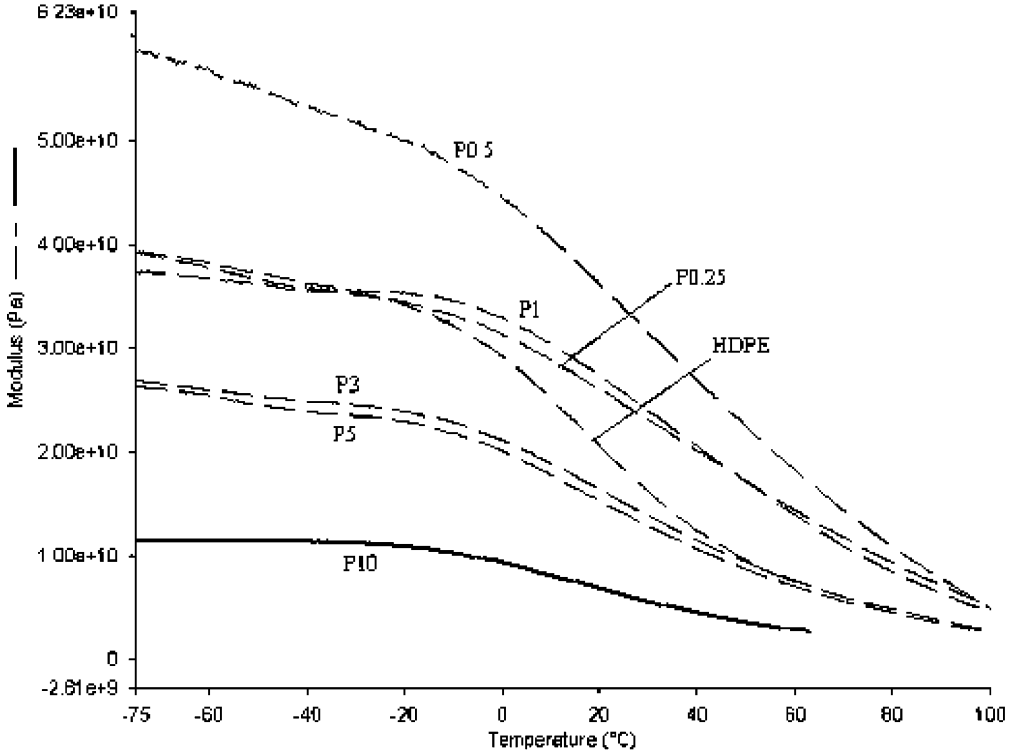

Figure 11. Storage modulus of HDPE and HDPE−POSS nanocomposite filaments.

At 190 and 200 °C, for the 10 wt % POSS sample, however, the slope in the low-frequency zone becomes positive. With increase in frequency, the slope first reaches a plateau (zero slope) and then becomes negative. As earlier discussed, from a rheological perspective this indicates a transition from meltlike to solidlike (critical gel) behavior. From Figure 10a,b it is evident that gelation starts at a POSS concentration between 5 and 10 wt %. The occurrence of the gelation in HDPE−POSS nanocomposites takes place at POSS concentration higher than 5 wt %.

The gelation may occur due to the following possibilities: (1) Strong particle−matrix interactions between molecularly/nanolevel dispersed POSS macromers and HDPE chains. This would hinder the chain mobility, causing the nanocomposites to behave in a solidlike way. (2) Finely dispersed POSS nanocrystals may themselves form a 3-D network, resulting in a solidlike behavior as is sometimes shown by concentrated suspensions.

From Figure 6a,b it can be seen that the complex viscosity increases with increase in POSS concentration at higher concentrations after an initial decrease at <1 wt % POSS content. Higher viscosity at higher POSS content may result from the formation of 3-D network of POSS nanocrystals in the HDPE matrix.

It is suggested that the interactions between the nanofiller particles and HDPE matrix are weak. This is evident from Figure 6a,b, where the viscosity values actually show a drop at low POSS concentrations (0.25 and 0.5 wt %). It is further suggested that POSS macromers are dispersed at the molecular/nanolevel at low concentrations and, due to their spheroidal shape, act as lubricant, only likely if particle−matrix interactive forces are weak. A similar behavior was reported by Kim et al.[10] with nanosilica−PEN (polyethylene 2,6-naphthalate) nanocomposites. Since both POSS and HDPE are essentially hydrophobic in nature, the forces acting between them are primarily weak van der Waals forces; with increase in POSS concentration beyond 0.5 wt %, POSS actually starts hindering the chain mobility by confinement of polymer chain segments. This may be because at increasing POSS concentration the segregated particle−particle interactions become more important than the weaker POSS−polymer interactions.

Dynamic Mechanical Analysis. The storage modulus of the HDPE−POSS nanocomposite monofilaments as a function of temperature is shown in Figure 11. It is clear from the figure that the storage modulus values for nanocomposites with low POSS loadings (0.25−1 wt %) are significantly higher, as compared to neat HDPE. With further increase in POSS content, the storage modulus values decrease. The highest storage modulus values are displayed by nanocomposite filaments with low POSS content (0.25−0.5 wt %). This is expected as the dynamic storage modulus also reflects the elastic component of the polymer, i.e., crystallization and orientation. Mathematically, it can be expressed as

$$G' = (\sigma_0/\gamma_0) \cos \delta \tag{9}$$

where G' is storage modulus, σ_0 and γ_0 are maximum amplitude of stress and strain, and δ is the phase lag between the stress and strain. The term cos δ depends on the mobility of the amorphous phase. The amorphous chain mobility gets restricted in HDPE−POSS nanocomposites probably at low POSS concentrations (0.25−0.5 wt %) due to POSS macromers occupying the free volume spaces in the amorphous regions, as they are dispersed at the molecular/nanolevel at low concentration levels. At low POSS concentrations (0.25−1 wt %), the nanocomposite filaments could also be drawn to a higher draw ratio and thus had higher orientation and crystallinity, which leads to the growing dominance of elastic component in nanocomposite filaments. It can also be seen that the drop in storage modulus of HDPE with temperature is sharper than the nanocomposites. This shows that nanocomposite filaments have improved thermomechanical properties as compared to neat

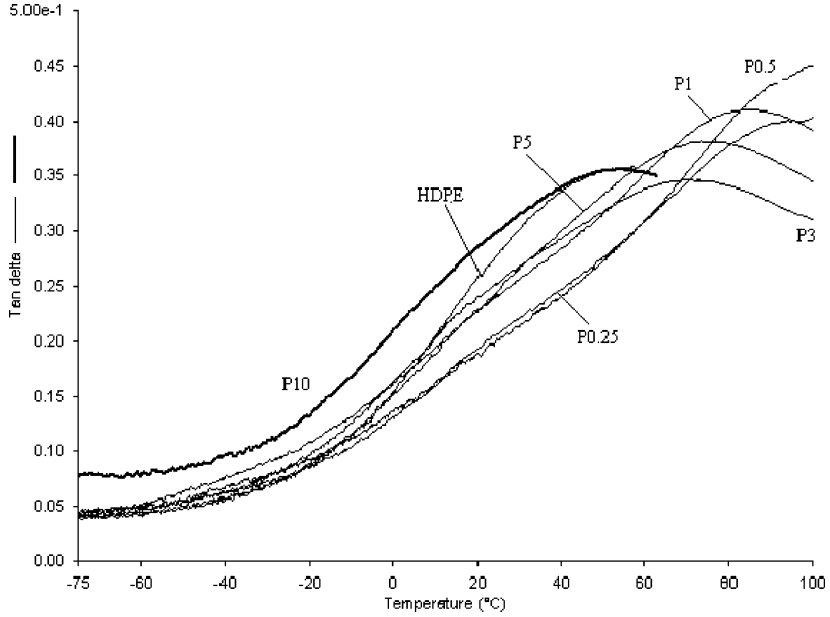

Figure 12. Loss tangent plots of HDPE and HDPE−POSS nanocomposite filaments.

HDPE. Figure 12 shows the plots of loss tangent (tan δ) as a function of temperature. The variation of loss tangent for neat HDPE and HDPE−POSS nanocomposite monofilaments with temperature shows distinct α-transition peaks in the temperature range 20−105 °C with peak maxima occurring in the temperature range 50−100 °C. It is observed that the intensity as well as the position (transition temperature value) of α-transition is higher for nanocomposites as compared to neat HDPE. The peak intensity increasing from 0.35 for neat HDPE to 0.4 and 0.45 for nanocomposites with 0.25 and 0.5 wt % POSS content, respectively. With further increase in POSS content a gradual decrease in peak intensity is observed. The α-transition peak position shows a similar trend (72, 94, and 103 °C for HDPE, 0.25 and 0.5 wt % POSS content). At POSS content of higher than 1 wt %, the intensity and position of α-peaks shift to lower values.

The occurrence of α-transition has been attributed to deformation of amorphous regions as a result of orientation within the crystallites[35] and deformation of chain segments within folds and loops of the interfacial regions.[36] Mandlekern[37] showed that the position of α-peak is inversely related to the lamella thickness in the crystalline region, and its intensity increases with the degree of crystallinity. Since in this study all the filaments are highly drawn and have high crystallinities (∼75%), it can be assumed that both HDPE and HDPE−POSS have primarily fringed fibrillar structure, which can be supported by the observation of some fibrillation occurring during tensile testing of monofilaments. The crystalline regions would thus consist primarily of fibrillar crystallites having parallel chains, and the shift in α-peak position and intensity is not attributed to lamella thickness and crystallinity. It is therefore proposed that the interphase plays a more significant role in the observed shift.

The β-peaks are not present in the tan δ curves of HDPE and HDPE−POSS nanocomposites. The absence of β-peaks in the tan δ plots is expected in such highly oriented systems. Even in unoriented polyethylene, β-transitions are barely discernible[38] and almost merge with α transitions. The molecular mechanism of β-transitions in polyethylenes is a controversial issue. Generally, the origin of β-transitions is attributed to three main phenomena: (1) diffusional motion of branch points, (2) relaxation of crystalline−amorphous interfacial components, and (3) glass−rubber transition of constrained amorphous components.

According to Mandlekern,[37] these transitions in polyethylene result from motions of disordered chain units in the interfacial regions. Sha et al.[39] tried to establish by their work that the β-transitions in polyethylenes are caused due to the glass transition phenomenon. HDPE generally does not display a glass transition due to its high crystallinity, which severely reduces the relaxation intensity and restricts mobility of chain segments in amorphous regions. This shifts the β-relaxations to higher temperatures, causing it to merge with α-peaks. Because of high orientation and crystallinity of HDPE−POSS nanocomposite systems, β-transitions are suppressed in the DMA traces.

Conclusions

Octamethyl-POSS is able to disperse homogeneously on a nano/molecular level in HDPE up to 1 wt % loading under shear conditions during melt mixing. However, at concentrations higher than 1 wt %, it crystallizes into nanocrystals, and at 10 wt % loading, it mostly exists as agglomerates. X-ray and DSC studies indicate that the presence of POSS does not change the crystallinity or crystal structure of HDPE up to 5 wt % loading; however, it affects the crystallization kinetics of HDPE and results in lowering of crystallinity and crystal perfection of HDPE at 10 wt %.

The complex viscosity at different angular frequencies suggests that the interactive forces between the POSS particles and HDPE matrix are primarily weak van der Waals forces. Using Cole−Cole and van Gurp analysis, it has been shown that POSS macromers are miscible in HDPE at low concentrations (upto 2 wt %). However, POSS becomes immiscible in HDPE at higher concentrations (>5 wt %) and at higher temperature, i.e., >180 °C. At low concentrations (0.25 and 0.5 wt %) POSS particles act as lubricants and lead to decrease in complex viscosity as compared to neat HDPE. With an increase in POSS concentrations, chain mobility is hindered and viscosity increases. Above 5 wt % POSS in HDPE, it forms a 3-D network of POSS nanocrystals which causes the system to exhibit solidlike (gelation) behavior at low shear rate ($\omega = 0.1$ rad/s). However, the strength of this network is poor, and it

breaks under moderate shear forces. The nanocomposites with low POSS content (0.25−0.5 wt %) show significantly high storage modulus and also enhanced thermomechanical properties than HDPE. The β-transitions are not recorded; however, the α-transition peaks are visible and occur at higher temperatures for all HDPE−POSS nanocomposites as compared to neat HDPE. This shift in alpha transition temperatures is attributed to the restriction of the movement of HDPE chain segments in the intercrystalline regions due to the presence of POSS macromers around the crystallite boundaries.

References and Notes

(1) Alexander, M.; Dubois, P. *Mater. Sci. Eng. Rep.* **2000**, *R28*, 1.
(2) Chazcau, L.; Cavailla, J. Y.; Canova, G. R.; Danclieval, R.; Boutherim, B. J. *Appl. Polym. Sci.* **1999**, *71*, 1797.
(3) Lee, A.; Lichtenhan, J. D. *Macromolecules* **1998**, *31*, 4970.
(4) Zheng, L.; Farris, R. J.; Coughlin, E. B. *Macromolecules* **2001**, *34*, 8034.
(5) Joshi, M.; Butola. B. S. *J. Macromol. Sci., Part C: Rev.* **2004**, *44*, 389.
(6) Fu, B. X.; Gelfer, M. Y.; Hsiao, B. S.; Phillips, S.; Viers, B.; Blanski, R.; Ruth, P. *Polymer* **2003**, *44*, 1499.
(7) Joshi, M.; Butola, B. S. *Polymer* **2004**, *45*, 4953.
(8) Larsson, K. *Ark. Kemi* **1960**, *16*, 209.
(9) Larsson, K. *Ark. Kemi* **1960**, *16*, 215.
(10) Kim, S. H.; Ahn, S. H.; Hirai, T. *Polymer* **2003**, *44*, 5625.
(11) Qian, J.; He, P.; Nile, K. *J. Appl. Polym. Sci.* **2004**, *91*, 1013.
(12) Liu, W.; Tian, X.; Cui, P.; Li, Y.; Zheng, K.; Yang, Y. *J. Appl. Polym. Sci.* **2004**, *91*, 1229.
(13) Waddon, A. J.; Petrovic, Z. S. *Polym. J.* **2002**, *34*, 876.
(14) Zheng, L.; Waddon, A. J.; Farris, R. J.; Coughlin, E. *Macromolecules* **2002**, *35*, 2375.
(15) Barry, A. J.; Dault, W. H.; Domicone, J. J.; Gilkey, J. W. *J. Am. Chem. Soc.* **1955**, *77*, 4248.
(16) Cho, K.; Lee, B. H.; Hwang, K. M.; Lee, H.; Choe, S. *Polym. Eng. Sci.* **1998**, *38*, 1969.
(17) Cho, K.; Tae-Kwang, A.; Park, I.; Lee, B. H.; Byung, H.; Choe, S. *J. Ind. Eng. Chem.* (*Seoul*) **1997**, *3*, 147.
(18) Kim, H. K.; Rana, D.; Kwag, H.; Choe, S. *Korea Polym. J.* **2001**, *8*, 34.
(19) Kwag, H.; Rana, D.; Choe, S. *J. Ind. Eng. Chem. (Seoul)* **2000**, *6*, 107.
(20) Kwag, H.; Rana, D.; Choe, K.; Rhee, J.; Woo, T.; Lee, B. H.; Choe, S. *Polym. Eng. Sci.* **2000**, *40*, 1672.
(21) Utracki, L. A.; Favis, B. D. Polymer Alloys and Blends. In *Handbook of Polymer Science and Technology*; Cheremisinoff, N. P., Ed.; Marcel Dekker: New York, 1989; Vol. 4.
(22) Utracki, L. A. In *Rheology of Polymer Alloys and Blends*; Hanser Publishers: Munich, 1989.
(23) Reichert, P.; Hoffmann, B.; Bock, T.; Thomann, R.; Mulhaupt, R.; Friendrich, C. *Macromol. Rapid Commun.* **2001**, *22*, 519.
(24) Chuang, H. K.; Han, C. D. *J. Appl. Polym. Sci.* **1984**, *29*, 2205.
(25) Han, C. D.; Chuang, H. K. *J. Appl. Polym. Sci.* **1985**, *30*, 4431.
(26) Han, C. D.; Kim. J. *J. Polym. Sci., Part B: Polym. Phys.* **1987**, *25*, 1741.
(27) Baek, D. M.; Han, C. D. *Polymer* **1995**, *36*, 4833.
(28) Wang, J.; Porter, R. S. *Rheol. Acta* **1995**, *34*, 496.
(29) Wasserman, S. H.; Graessley, W. W. *Polym. Eng. Sci.* **1996**, *36*, 852.
(30) Stachurski, Z. H. Melt Properties and Solidification. In *Polymer Update: Science and Engineering*; Cook, W. D., Guise, G. B., Eds.; Australian Polymer Science Series Vol. 2; Polymer Division, RACI, 1989.
(31) Winter, H. H.; Chambon, F. *Polym. Bull. (Berlin)* **1985**, *13*, 499.
(32) Vilgis, T. A.; Winter, H. H. *Colloid Polym. Sci.* **1988**, *266*, 494.
(33) Gelfer, M. Y.; Winter, H. H. *Macromolecules* **1999**, *32*, 8974.
(34) Winter, H. H.; Chambon, F. *J. Rheol.* **1986**, *30*, 367.
(35) Boyd, R. H. *Polymer* **1985**, *26*, 1123.
(36) Khanna, Y. P.; Turi, E. A.; Taylor, T. J.; Vicroy, V. V.; Abbott, R. F. *Macromolecules* **1985**, *18*, 1302.
(37) Popli, R.; Glotin, M.; Mandlekern, L.; Benson, R. S. *J. Polym. Sci., Part B: Polym. Phys.* **1984**, *22*, 407.
(38) Razavi-Nouri, M.; Hay, J. N. *Polymer* **2001**, *42*, 8621.
(39) Sha, H.; Zhang, X.; Harrison, I. R. *Thermochim. Acta* **1991**, *192*, 233.

MA051357W